



RESEARCH ARTICLE

Multi-scale drivers of spatial patterns in floodplain sediment and phosphorus deposition

Rebecca M. Diehl¹  | Kristen L. Underwood² | Shayla P. Triantafyllou³ | Don S. Ross⁴ | Stephanie Drago⁵ | Beverley C. Wemple¹ 

¹Department of Geography and Geosciences, University of Vermont, Burlington, Vermont, USA

²Department of Civil and Environmental Engineering, University of Vermont, Burlington, Vermont, USA

³Department of Geosciences, Colorado State University, Fort Collins, Colorado, USA

⁴Department of Plant and Soil Science, University of Vermont, Burlington, Vermont, USA

⁵USDA NRCS Vermont, Colchester, Vermont, USA

Correspondence

Rebecca M. Diehl, Department of Geography and Geosciences, University of Vermont, Burlington, VT 05405, USA.
Email: rebecca.diehl@uvm.edu

Funding information

Lake Champlain Basin Program; Vermont Department of Environmental Conservation; University of Vermont Gund Institute on the Environment; The Nature Conservancy Vermont; National Science Foundation

Abstract

The capacity for floodplains to capture sediment and filter pollutants is spatially variable and depends on the complex interactions of geomorphic, geologic, and hydrologic variables that operate at multiple scales. In this study, we integrated watershed-scale and local assessments to improve our understanding of floodplain depositional patterns. We developed a dataset of event-scale observations of sediment and phosphorus deposition rates distributed at 129 plots across large environmental gradients of floodplain topography, valley geometry, and watershed characteristics in the Lake Champlain Basin, Vermont. Plot-scale observations were used to evaluate the cross-scale influence of environmental factors and were summarized into site-scale averages to explore regional trends. Consistent with other studies, floodplain deposition generally scaled with drainage area, but trends were longitudinally discontinuous and depended on variations in valley width and slope. While variability in deposition patterns at the watershed-scale was large (average of 2.0 (0.2–9.8) kg sediment m⁻² yr⁻¹; average of 1.4 (0.2–6.5) g phosphorus m⁻² yr⁻¹), the range in deposition rates locally across a floodplain was greater (average of 4.6 (0.06–21.7) kg sediment m⁻² yr⁻¹; average of 6.4 (0.1–41.1) g phosphorus m⁻² yr⁻¹). Local variables that described the proximity to water and sediment sources, and frequency with which the plot was activated by a flood, had the greatest relative contribution to boosted regression tree models of phosphorus deposition rates, highlighting the importance of river–floodplain connectivity for floodplain functioning and the profound impact of human activities that limit such connectivity. Patterns identified in our study may guide prioritization of restoration and conservation practices designed to capture sediment and phosphorus on floodplains.

KEYWORDS

hydrologic connectivity, restoration, water quality, watershed

1 | INTRODUCTION

Floodplains perform numerous functions that support ecosystem services (Opperman et al., 2010), including the mitigation of water-related hazards (Gourevitch et al., 2020), improvement of water quality (Wohl, 2021), and provisioning of riparian and aquatic habitats that support some of the most biodiverse settings in the world (Ward et al., 1999). Increasingly, floodplains are recognized as an important

component of watershed management plans aimed at mitigating degraded water quality in receiving waters, such as excess nutrient runoff contributing to harmful algal blooms (Gordon et al., 2020; Tschikof et al., 2022). Floodplains can be leveraged for their storage of sediment and nutrients, to reduce downstream flux of these constituents (Johnson et al., 2016; Noe & Hupp, 2005; Noe et al., 2022). When well connected to their rivers, floodplains can be targeted for conservation to preserve this function and, where historic land uses

This is an open access article under the terms of the [Creative Commons Attribution](https://creativecommons.org/licenses/by/4.0/) License, which permits use, distribution and reproduction in any medium, provided the original work is properly cited.

© 2022 The Authors. *Earth Surface Processes and Landforms* published by John Wiley & Sons Ltd.

have reduced river–floodplain connection, floodplains may be restored to enhance their storage capacity (Opperman et al., 2009; Tockner et al., 1999). To best focus conservation or restoration efforts in a watershed, river managers need to know where floodplains can be most effective at attenuating watershed fluxes and maximizing sediment and nutrient retention from floodwaters.

In this paper we explore spatial patterns of modern (i.e., recent decades) sediment and sediment-bound nutrient deposition, important for understanding the impact of watershed management actions. Over longer timescales, depositional and erosional processes define the net storage of sediment in floodplains and determine their current distribution and morphology (Church, 2002; Jain et al., 2008; Wohl, 2021). This structural organization influences the strength of hydrologic and sediment connections (i) between floodplains and the upstream watershed (longitudinal), (ii) between floodplains and the adjacent river channel (vertical), and (iii) across the floodplain (lateral) (Ward, 1989; Wohl et al., 2019). The stronger these connections, the more efficient is the transfer of water and sediment, and the greater the expected deposition in floodplains (Bartsch et al., 2022; Opperman et al., 2009; Tockner et al., 1999). The relationship between floodplain structural organization and connectivity that influences deposition can be characterized at various spatial scales.

At the watershed scale, total floodplain deposition increases with watershed area as rivers and their floodplains increase in size (Magilligan, 1985; Swinnen, Daniëls, et al., 2020). However, longitudinal variation in valley width from changes in lithology and bedrock characteristics, relict glacial deposits, or geologic structures (Wohl, 2021) results in wider segments with a lower gradient and high sediment retention interspersed with steep, laterally confined segments where there is little space to accommodate floodplain deposition (Stanford et al., 1996; Wohl et al., 2018). Trends in sediment storage and deposition also vary within and between watersheds because of hydrologic and sediment regimes that influence the longitudinal connectivity, and determine the timing, concentration, and volumes of sediment supplied (Wohl et al., 2015).

At the valley scale, trends in deposition may be described by the geometry of the channel and floodplain, which influences the strength of the connection between floodwaters and the floodplain. Wider floodplains capture greater volumes of sediment, but deposition is also greater, on a per area basis in wider valleys (Hupp et al., 2013). Shallower channels, or those with lower bank heights relative to floodplain widths, tend to have greater river–floodplain connectivity and higher deposition rates (Schenk et al., 2013), although high, unstable banks may also locally enhance sediment loads, leading to elevated deposition rates (McMillan & Noe, 2017). While some have documented a negative relationship between channel gradient and deposition (Hupp et al., 2013; Schenk et al., 2013), deposition rates have also been correlated with sediment loads, a function of gradient and the river's transport capacity (Gellis et al., 2008).

At the local scale, floodplain topography and landcover influence the routing of floodwaters that disperse sediment across the floodplain (Middelkoop & Asselman, 1998). Areas that are highly connected to sediment-laden floodwaters have high deposition rates that decrease rapidly with distance (Hupp et al., 2015; Pizzuto et al., 2008). Elevated deposition has been associated with areas closer to the river or floodplain channel (Swanson et al., 2008), lower

on the floodplain (Hupp & Bazemore, 1993; Kleiss, 1996), or inundated the most frequently (Hupp et al., 2008), and can be associated with distinct geomorphic surfaces (Kaase & Kupfer, 2016; Steiger & Gurnell, 2003). Vegetation growing on floodplains can interrupt flow patterns, enhancing deposition within some plant communities (Olde Venterink et al., 2006), introducing micro-topography (Temmerman et al., 2005), and altering seasonal depositional patterns (Brunet & Astin, 1998).

Rivers, however, are complex systems governed by interactions among variables operating across these spatial scales, resulting in nonlinear or threshold patterns (Phillips, 2003; Soranno et al., 2014). Human modifications to the landscape exacerbate the complexity of cross-scale interactions, variably altering hydrologic and sediment connectivity depending on the type, extent, and intensity of the activities (De Vente et al., 2007; McCluney et al., 2014). For example, sediment supplies are governed by watershed geologic and land use characteristics, which in turn influence sediment loads and deposition patterns (Gellis et al., 2008). Yet the caliber and nature of the sediment supplied also influence floodplain typology, as described by Nanson and Croke (1992), determining the strength and distribution of floodwater connectivity across the floodplain.

To understand the spatial variability of deposition patterns, it is therefore necessary to take a cross-scale perspective. McMillan and Noe (2017) demonstrated these cross-scale patterns within a limited geographic scope. In five small urban watersheds in the Southeastern USA, they found that lateral connectivity influenced the retention of sediment and nutrients, but that deposition rates depended on the location along the stream network. The relative importance of—and interactions among—the structural organization, connectivity, and the human impact on deposition remain relatively understudied, notably across a larger range of spatial scales and for a variety of land uses.

The goal of this paper was to characterize the cross-scale interactions manifesting in variable spatial patterns of floodplain deposition across a broad range of environmental conditions, with a particular focus on metrics of longitudinal–vertical–lateral (dis)connectivity resulting from post-glacial and human-caused channel and floodplain disturbance. We collected sediment and sediment-bound phosphorus observations at the plot scale (10^0 m²) that capture variability in local floodplain topography and connectivity and aggregated it to develop a site-scale (10^2 – 10^3 m²) dataset that captures a range of valley- and watershed-scale characteristics. With this nested dataset, we applied machine learning techniques that are well adapted for identifying threshold and nonlinear relationships characteristic of complex Earth systems (Bergen et al., 2019) to investigate which factors, over which scales, are important for describing observed deposition patterns. We worked in the Lake Champlain Basin of Vermont in the northeastern USA, where the US Environmental Protection Agency has set a Total Maximum Daily Load target of 34% reduction in phosphorus export to the lake (EPA, 2016) and where phosphorus loading to the lake is dominated by particulate forms, notably during larger floods (Vidon et al., 2018). The region has a complex glacial and human land use history that has variably disconnected floodplains from their rivers (Kline & Cahoon, 2010). Disconnected floodplains likely contribute to degraded water quality (Langendoen et al., 2012), and improving river–floodplain connectivity may help to capture sediment and sediment-bound phosphorus.

2 | METHODS

2.1 | Study area and design

To evaluate the spatial patterns of floodplain deposition across a large environmental gradient, we developed a regional dataset of sediment and sediment-bound phosphorus for the Lake Champlain Basin (LCB; 12,000 km²) in the Northeastern USA, which drains much of western Vermont and includes part of eastern New York and southern Quebec (Figure 1). In Vermont, the basin spans six diverse physiographic regions (Stewart & MacClintock, 1969), from the relatively wet (127 cm yr⁻¹) and forested Northern Green Mountains dominated by northern hardwoods to the dryer (81 cm yr⁻¹) Champlain Valley dominated by agriculture along low-relief plains (Randall, 1996). While annual floods on the rivers that drain to Lake Champlain occur predominantly from spring snowmelt, with nearly one-half of the annual streamflow concentrated in a 6- to 8-week period, fall and early winter storms are responsible for a second mode of less common, but intense floods (Collins et al., 2014; Shanley & Denner, 1999).

Rivers and floodplains in the region have been affected during the past few centuries as a result of ongoing postglacial, isostatic rebound of Vermont landforms and a history of land use impacts (Stewart & MacClintock, 1969; Underwood et al., 2021). Uplands cleared for logging and agriculture resulted in increased flooding and encroachment, which led to management actions such as dredging, channelization, berm building, and wood removal, which altered the river channels and floodplains (Kline & Cahoon, 2010). Elevated levels of phosphorus, from a long history of land clearing and associated soil erosion and agricultural practices, along with current land uses, have degraded water quality (Isles et al., 2015; Smeltzer et al., 2012).

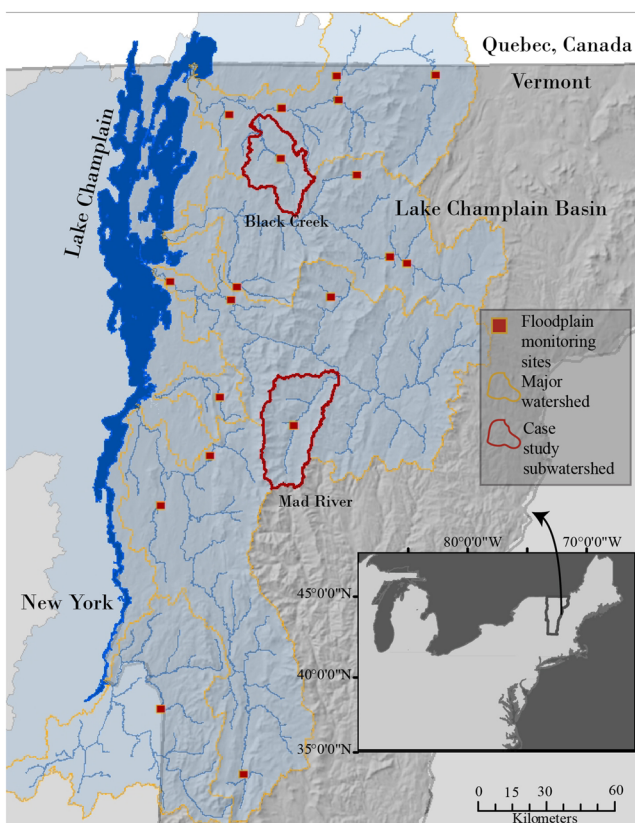


FIGURE 1 Map of Lake Champlain Basin, Vermont [Color figure can be viewed at wileyonlinelibrary.com]

We established a floodplain monitoring network located within the six major watersheds in the Vermont portion of the LCB. Nineteen sites were located on streams draining from 10 km² to 2800 km² (Figure 1). These sites were chosen to capture a range of watershed- to valley-scale controls on floodplain sediment and phosphorus deposition and represent hydroclimatic, geologic, and topographic gradients, as well as differing upstream land use and land cover characteristics (Medalie et al., 2012; Underwood et al., 2017; Table 1). We located sites in areas of the watershed where sediment accumulation is likely to occur, determined by each site's position on a drainage area-slope plot, often used to identify major transitions in river character and behavior (Church, 2002; Jain et al., 2008; Sklar & Dietrich, 1998) (Figure 2). Approximately half of the floodplains are considered low energy and half medium energy, based on the Nanson and Croke (1992) classification, indicative of differences in form and depositional processes. We chose floodplains with moderate to full vertical connection to the river, as measured by the degree of channel incision (i.e., incision ratio less than 1.6), to assure inundation during the study period, although one site had an incision ratio greater than 1.6. See Section 2.3 and Supporting Information Figure S2 for the definition of incision ratio. We then sited monitoring plots (3–12 per site, total of 140) across topographic and hydrologic gradients at each site to represent local controls (Figure 3). Each plot consisted of four 15 × 15 cm square artificial turf pads (8 mm bristles) spaced orthogonal to each other, 1 m from a central bamboo pole (Figure 3).

In addition to exploring the cross-scale controls on deposition across the Lake Champlain Basin, we performed a scenario analysis on two contrasting headwater watersheds to evaluate how an understanding of the spatial patterns of deposition can inform watershed management plans that target improved floodplain functioning to mitigate poor water quality (Figure 1). Absent human impacts, we assumed that floodplains in our study may achieve full vertical and lateral hydrologic connectivity with floodwaters, defined as no incision and regular inundation. Black Creek (BC) drains 230 km² of predominately forested land (70%), with 9% wetland cover, in the Missisquoi River Watershed in northern Vermont. Due to wide, flat valleys, 40% of the river corridor is cultivated or managed as pasture. The Mad River (MR), a slightly larger watershed (368 km²), is in the headwaters of the Winooski River Watershed in central Vermont. The watershed is largely forested (87%), with less wetland cover (3.7%), and has less agriculture through the river corridor (17%). Reaches in the Mad River watershed are steeper than those in Black Creek (MR mean = 0.03 and SD = 0.03; BC mean = 0.007 and SD = 0.008; $t[226] = 5.16$, $p < 0.001$), and their channels are more incised (MR mean = 1.5 and SD = 0.37; BC mean = 1.3 and SD = 0.29; $t[226] = 2.09$, $p = 0.04$).

2.2 | Sediment and phosphorus deposition dataset

Turf mat plots installed in the summer of 2019 were monitored for flood-deposited sediments for 2 years. Following individual flood events, turf mats were evaluated for evidence of inundation and deposition, excavated, and collected, and replaced with new pads. Sediments were dried and weighed to identify event-scale deposition (Dep ; kg m⁻²), which generally refers to both sediment and phosphorus deposition. To build a dataset of phosphorus concentrations at the plot

TABLE 1 Environmental characteristics used to evaluate variability in floodplain deposition, measured for each site (watershed and valley) and plot (local)

Representative scale	Characteristics		Median	Min.	Max.
Watershed	Drainage area (km ²)	DA	184	10	2,745
	% Watershed in wetland	WS _{WET}	7%	3%	17%
	% Watershed in agriculture	WS _{AG}	9%	<1%	47%
	% Watershed in development	WS _{DEV}	1.4%	<1%	2.50%
	% Watershed with HSGD ^a	WS _{HSGD}	54%	26%	84%
Valley	Slope (m m ⁻¹)	S	0.0009	0.00001	0.0063
	Specific streampower (W m ⁻²)	SSP	37.2	0.8	137
	Incision ratio	IR	1.2	1	1.9
	Floodplain width ^b (m m ⁻¹)	W _{FP}	12.0	2.2	35.1
Local	Distance from channel ^b (m m ⁻¹)	D	0.47	0.01	4.8
	Annual inundation probability	Inun	0.46	0.01	1.0

^aHydrologic soil group D (HSGD) are soils with high runoff potential.

^bNormalized by channel width.

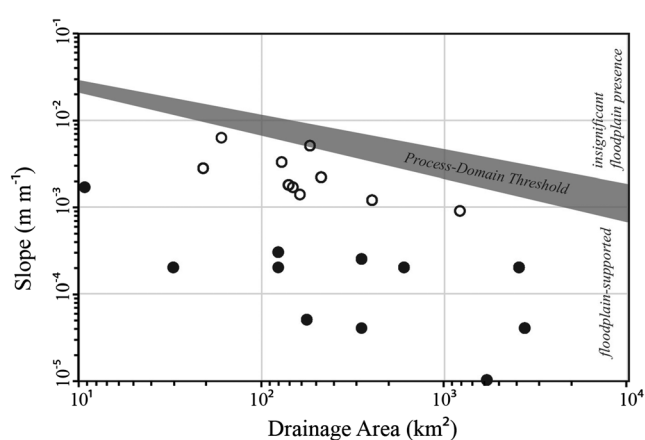


FIGURE 2 Nineteen study sites plotted on drainage area–slope plot. All sites fall below the threshold identified by Jain et al. (2008), as a general determinant of shift in process domain. Open circles indicate sites classified as “medium energy” and closed circles as “low energy” according to Nanson and Croke (1992)

scale, samples from two of the four mats within each plot were composited into one sample. The sample was sieved (2 mm) and ground to pass a 0.5 mm sieve. A representative 0.5 g subsample was analyzed for total phosphorus using a microwave-assisted nitric acid digest following EPA method 3050B (US EPA 1996). Digests were analyzed for total phosphorus by ICP-OES (Avio 300, Perkin Elmer Corp, Norwalk, CT, USA). Total phosphorus concentrations (P_{conc} ; mg kg⁻¹) of the analyzed sediment were used to convert sediment deposition (Sed_Dep ; kg m⁻²) to phosphorus deposition (P_Dep ; g P m⁻²).

To aggregate deposition measurements at a single plot resulting from multiple flood events during the study period, we defined an annual deposition rate that accounts for the variability in the magnitude of observed flood events. In any given year, the annual probability, p , of a flood event of a defined recurrence interval occurring is $1/T$, where T equals the expected recurrence interval (see the second-to-last paragraph in this section for more information). Because these flood events are independent of each other, multiple flood events can occur in a single year. To estimate the annual deposition rate (Dep_{yr} ; kg m⁻² yr⁻¹), we integrated the deposition associated with observed flood events at each plot, with respect to p :

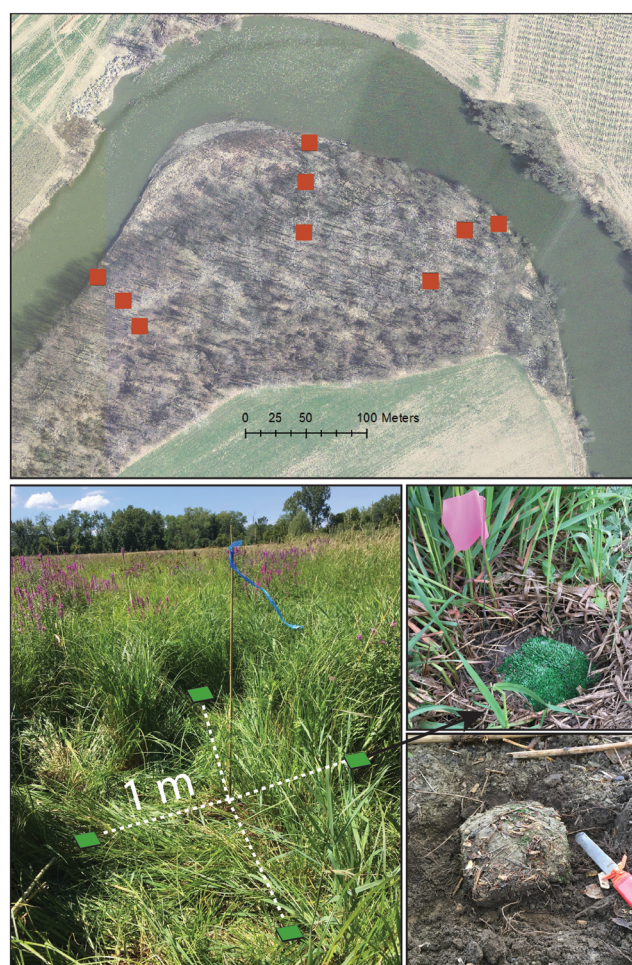


FIGURE 3 Example of a typical site (top), with transects of monitoring plots (orange squares). Each monitoring plot (bottom, left) consists of four 15 × 15 cm turf mat pads (green squares), 1 m from a central pole. Following inundation, we excavated each pad (bottom, right) for analysis [Color figure can be viewed at wileyonlinelibrary.com]

$$Dep_{yr} = \int_0^1 Dep(p) dp \quad (1)$$

Based on the methods in Olsen et al. (2015), we solved the integral using the trapezoidal rule (Equation 2). In this equation, j represents the flood recurrence interval:

$$Dep_{yr} = \sum_j \frac{[(p_{j+1} - p_j)(Dep_{p_{j+1}} + Dep_j)]}{2} \quad (2)$$

Because each plot had between one and three observations associated with flood events of a range of recurrence intervals, we extrapolated the observations by assuming that the relationship between recurrence interval and deposition approximated a logarithmic function. If the plots at a site were only inundated once during the study period, we assumed that the 1-year flood ($p = 1.0$) deposited 0 kg m^{-2} . Similarly, if some plots experienced inundation and deposition during a flood, while other plots at the same site did not, we assigned a deposition value of 0 kg m^{-2} to those plots not inundated.

To identify the recurrence interval of each flood event, we related relevant site and storm characteristics (e.g., drainage area, basin outlet coordinates, precipitation total) at each ungauged site to nearby USGS stream gages, where flood frequency curves have been developed (see Olson, 2014). For each flood event, we downloaded interpolated maps of observed precipitation totals measured by the National Weather Service (NOAA, 2021a) and of modeled snow water equivalent values from the National Snow and Ice Data Center (NOAA, 2021b), and calculated basin average precipitation totals for each site affected by that flood. Basin average precipitation totals were used to scale measured discharge, and the associated flood frequency, at USGS gages to the ungauged sites.

From plot-scale Dep_{yr} observations of sediment and phosphorus, we calculated a floodplain-average deposition value (Dep_{site} ; $\text{kg m}^{-1} \text{ yr}^{-1}$), which represents the likely total annual deposition of sediment and phosphorus per length of river. Trends in the annual deposition rate for each plot and the distance from the stream channel, commonly understood to have an exponential decay (e.g., Walling & He, 1998), were used to determine the relationship between distance and deposition for the 100-year floodplain, along one valley side. A unique relationship between Dep_{yr} and distance was developed for each of the 19 sites. We used this relationship to interpolate deposition across the site, aggregating across the floodplain to calculate the floodplain-average deposition.

2.3 | Watershed, valley, and local characteristics

We identified a suite of characteristics with potential for influencing spatial variability in sediment and sediment-bound phosphorus sourcing and deposition at the watershed and valley setting of each floodplain site, and additional characteristics that may be important for describing local variability in deposition among plots (Table 1). At the watershed scale, we calculated the drainage area (DA) and the percent of the upstream watershed with soils in hydrologic soil group D that have high runoff potential (WS_{HSGD} ; USDA 1986), and whose land cover is classified as wetlands (WS_{WET}), impervious (WS_{IMP}), or agriculture (WS_{AG} ; Vermont Center for Geographic Information, 2018). Land use and cover data provide insight into sources of sediment and phosphorus as well as the longitudinal connectivity of the watershed. The potential for storing water (i.e., high WS_{WET} or low WS_{HSGD}) or accelerating runoff (i.e., high WS_{IMP} or WS_{AG}) may influence hydrograph shapes and sediment regimes and may be important for understanding nutrient runoff.

At the valley scale, we identified channel slope (S) adjacent to a site, measured from a LiDAR-derived DEM (0.7 m resolution QL2;

Vermont Center for Geographic Information, 2019) for a reach that was no less than 10 channel widths long and had no significant breaks in elevation (i.e., relatively consistent slope). Specific stream power (SSP) in this reach was calculated as $Q_2 \times S \times 9810$, using the discharge of the 2-year flood (Q_2 ; Olson, 2014). We characterized the 100-year floodplain width (based on Diehl, Gourevitch, et al., 2021) as a ratio (W_{FP}) expressed relative to channel width measured from air photos and the DEM. Additionally, we identified a channel incision ratio (IR), defined as the ratio of the floodplain low-bank height, indicative of the historical floodplain, to the bankfull depth defined as the flow at the 1.5-year recurrence interval (Beechie et al., 2008; Kline et al., 2009) (Supporting Information Figure S1). Values less than 1.3 indicate low incision and regular access of floodwaters to the floodplain, whereas values greater than 1.6 indicate significant incision and low connectivity with floodwaters. Where available, field-measured data from Vermont stream geomorphic assessments were used (Vermont Agency of Natural Resources, 2021). Otherwise IR values were estimated from LiDAR-derived DEMs (Palaseanu-lovejoy et al., 2016). We note that within a given site, W_{FP} and IR may vary among the plots because of cross-sectional differences.

At the local scale, we measured the nearest distance (D) of each plot from the edge of the river channel (normalized by channel width). We also identified the annual likelihood of inundation ($Inun$) for each plot—a measure of the lateral connectivity, derived from a dataset of probabilistic floodplain maps developed for the Lake Champlain Basin from LiDAR-derived DEMs (Diehl, Gourevitch, et al., 2021). Using a low-complexity mapping approach these maps were created to identify the likely inundation extent of a range of recurrence interval floods, from the 2- to 500-year flood. From this dataset, we created a composite map of annual inundation probabilities (Diehl, Wemple, et al., 2021). We note that even though the floodplain maps did not identify the threshold between floods that occur once every 2 years and those that occur more frequently, annual flood observations allowed for modifications to $Inun$ when $Inun > 0.5$.

2.4 | Data analyses

We first evaluated simple bivariate trends in the plot-scale dataset, calculating the Spearman rank correlation between the physical characteristics of the watershed, valley, and local floodplain, and field-measured values of sediment and sediment-bound phosphorus concentrations (Sed_Dep , P_conc ; Table 1).

2.4.1 | Boosted regression trees (BRTs)

We then used a BRT modeling approach: (1) to analyze the key variables driving annual plot-scale phosphorus deposition rates (P_Dep_{yr}) and reduce the dimensionality of our dataset in order to highlight the most important drivers of floodplain deposition and understand their relationships; and (2) to predict P_Dep_{yr} for a scenario analysis within two watersheds. We developed two distinct models to achieve these objectives, as described below.

The BRT is a powerful, ensemble method for exploring data from complex, nonlinear systems with many, sometimes correlated, predictor variables that interact across multiple scales. BRTs are particularly

well suited for analysis and prediction in complex problem domains because they are flexible (e.g., handle missing data and multiple types of data with non-normally distributed residuals) and inherently consider interactions among factors (Elith et al., 2008; Pittman et al., 2009). BRTs combine regression trees with boosted machine learning to adaptively improve model performance (Elith et al., 2008). The boosting technique builds hundreds to thousands of statistical trees that iteratively fit the residuals of prior trees. As a result, BRTs provide an estimate of the relative importance of each predictor variable to explain variation in the dependent variable and partial dependence plots that communicate the effect of each predictor variable after accounting for the average effects of all other variables in the model. The relative influence of predictor variables is based on the number of times that variable is selected for splitting (e.g., added to the model), weighted by the squared improvement to the model resulting from each split, and averaged over all trees. We executed the BRT model with the DISMO package in R (Hijmans et al., 2015) following the guidelines of Elith et al. (2008). Because of a relatively low sample size ($n = 128$), we raised the default bag fraction of 0.5 to 0.6, where 60% of the sample is drawn at random, without replacement, from the full training set at each iteration. Tree complexity and learning rate were optimized based on model predictive performance during validation using cross-validation.

In the first BRT model, we evaluated the best drivers of P_Dep_{yr} , from the suite of physical characteristics identified for this study (Table 1). After initial model calibration with all input parameters, subsequent model simplification successively dropped those parameters that contributed the least to total error prediction. Once all variables had more than 3% relative influence, we then removed the correlated predictors (Spearman rank correlation coefficient > 0.7) with the lower influence to prevent overfitting of the model.

We developed a second, simpler, BRT model to use as a predictive tool in the scenario analysis. From the top variables identified in the first model, we kept those variables that had more than 10% relative influence, and specifically included IR and $Inun$ to assure characterization of vertical and lateral hydrologic connectivity. To remove some of the noise in the data, and better understand trends in deposition, we classified the variables based on thresholds evident in the partial dependence plots of the first model.

2.4.2 | Predicting existing and potential phosphorus deposition

We applied the predictive BRT model to the Black Creek and Mad River watersheds (Figure 1) and calculated average annual floodplain deposition rates ($g\ P\ m^{-2}\ yr^{-2}$) at the reach scale, for reaches with a DA up to $25\ km^2$ (i.e., $10\ mi^2$, to match flood inundation maps; Diehl, Gourevitch, et al., 2021) that met the DA -slope threshold indicative of settings that support floodplains (Figure 2). Because we expect that floodplain deposition depends on distance from the river channel, we calculate a spatial average for each reach, integrating across the full 100-year floodplain based on the modeled relationship between distance from the channel and annual deposition.

We applied the model for two scenarios: existing and potential conditions. The existing scenario used current values, including measured IR and $Inun$ values. The potential scenario assumed full connectivity, defined as no incision and frequent inundation, representative of

a fully functioning floodplain, or one that may be achieved absent human impacts. For the potential scenario, we used updated IR ($IR = 1.0$) and $Inun$ values. We shifted the median annual probability of inundation based on the shift in the IR , assuming that, by restoring vertical connectivity, the lateral connectivity would also improve. The change in $Inun$ scaled with the change in IR and was based on observations from the existing relationship between IR and median $Inun$ in the study watersheds (Supporting Information Figure S2). We acknowledge that this approach does not account for all lateral constraints nor improvements to land cover and topography that also may enhance connectivity and change deposition patterns, and that disconnectivity can also exist without anthropogenic perturbations, such as from landslides or in response to base-level shifts (Schumm, 1999).

3 | RESULTS

3.1 | Inundating floods and floodplain deposition rates

We measured deposition following six localized and one widespread flood event (Table 2). Localized flooding occurred because of spring snowmelt and rain on snow events in 2021 and convective storms in 2019 and 2021. Heavy rainfall on October 31 to November 1, 2019 resulted in significant flooding across the study area. Flood events had recurrence intervals that ranged from 1 to 130 years. Floods that occurred in the winter and early spring scaled to watershed-average snow water equivalent, while those that occurred because of localized rain were a function of watershed-average precipitation. Because the 1 November rainstorm and resulting flooding had a geographic signature (e.g., greater precipitation in the north and along the western portion of the state), we also found high predictive capability for determination of the recurrence interval based on location (Table 2 and Supporting Information Table S1).

We collected 188 unique observations of sediment and phosphorus deposition, which occurred on 129 turf mat plots (out of 140) at 19 sites. Of the remaining 11 plots, eight were not inundated during the study period and three were not relocated. Erosion was noted around four plots, and three plots were either partially or fully eroded through bank retreat. We assigned these instances a value of “0” $kg\ m^{-2}$ in the dataset.

Field-measured sediment and phosphorus deposition (Sed_Dep and P_Dep) varied by three and two orders of magnitude, respectively (Table 3). Measured concentrations of phosphorus in sampled sediments were less variable than deposition rates, although some samples had relatively low phosphorus concentrations (e.g., $426\ mg\ kg^{-1}$), while others were notably elevated (e.g., $1506\ mg\ kg^{-1}$). Accounting for flood frequency, annual sediment and phosphorus deposition at the plot scale ranged from 0.06 to $21.7\ kg\ m^{-2}\ yr^{-1}$ and from 0.1 to $41.1\ g\ P\ m^{-2}\ yr^{-1}$, respectively. Sediment deposition was negatively correlated with P concentration ($\rho = -0.23$; $p < 0.01$). Sediment deposition rates explained 95% of the variability in phosphorus deposition rates ($p < 0.001$). Because of this close correlation in sediment and phosphorus deposition, and the overall importance of phosphorus in driving algal blooms in freshwater systems, we focused the analyses of general trends on phosphorus deposition rates.

Extrapolated to the site scale for the full 100-year floodplain width, based on within-site trends, Sed_Dep_{yr} and P_Dep_{yr} averaged

TABLE 2 Summary of flood events that inundated at least one of the 19 study sites, resulting in measurable deposition

Flood Date	Mechanism	# of sites Inundated	# of plots collected	Estimated flood recurrence interval
June 20, 2019	Rain	1	7	<5-year
October 17, 2019	Rain	2	13	<10-year
November 1, 2019	Rain	19	128	1.5- to 130-year
December 25, 2020	Rain	5	9	<2-year
March 11, 2021	Snowmelt	1	1	<5-year
March 26, 2021	Rain and snowmelt	6	16	<5-year
May 1, 2021	Rain	2	14	<5-year

TABLE 3 Sediment and phosphorus deposition measured during the study period

		Units	Median	Min.	Max.	Avg.	SD
Plot-scale field measures							
Sediment deposition	<i>Sed_Dep</i>	kg m ⁻²	8.5	0.3	162	17	21.5
Phosphorus concentration	<i>P_conc</i>	mg kg ⁻¹	723	426	1506	751	214
Phosphorus deposition	<i>P_Dep</i>	g P m ⁻²	5.7	0.3	82	11.9	14.4
Plot-scale annual deposition							
Sediment deposition rate	<i>Sed_Dep_{yr}</i>	kg m ⁻² yr ⁻¹	2.5	0.06	21.7	4.6	4.9
Phosphorous deposition rate	<i>P_Dep_{yr}</i>	g P m ⁻² yr ⁻¹	3.7	0.1	41.1	6.4	7.2
Site-scale annual deposition							
Sediment deposition rate	<i>Sed_Dep_{yr}</i>	kg m ⁻² yr ⁻¹	0.9	0.2	9.8	2.0	2.5
Phosphorus deposition rate	<i>P_Dep_{yr}</i>	g P m ⁻² yr ⁻¹	0.7	0.2	6.5	1.4	1.7
Floodplain sediment deposition	<i>Sed_Dep_{FP}</i>	kg m ⁻¹ yr ⁻¹	156	7.5	1098	249	275
Floodplain phosphorus deposition	<i>P_Dep_{FP}</i>	g P m ⁻¹ yr ⁻¹	147	6.8	637	198	187

2.0 kg m⁻² yr⁻¹ and 1.4 g P m⁻² yr⁻¹, respectively. As a result, at the 19 sites, *Sed_Dep_{FP}* and *P_Dep_{FP}* averaged 249 kg m⁻¹ yr⁻¹ and 198 g P m⁻¹ yr⁻¹ (Table 3).

3.2 | Multi-scale controls on spatial patterns of floodplain deposition

Sediment deposition (*S_Dep*) and phosphorus concentration (*P_conc*) were correlated with environmental variables at multiple scales. A watershed's land use and land cover characteristics were important for both sediment deposition and phosphorus concentrations. *WS_{WET}* was negatively correlated with *S_Dep*, and *WS_{HSGD}*, *WS_{AG}*, and *WS_{IMP}* were positively correlated with *P_conc* (Table 4). Slope and specific stream power, which are indicators of the potential energy expenditure, were positively correlated with *S_Dep* and negatively with *P_conc*. Locally we found that plots further from the channel had greater *P_conc* but smaller *S_Dep*.

When multi-scale characteristics were evaluated together in the BRT model to describe variability in annual plot-scale phosphorus deposition (*P_Dep_{yr}*), local controls had the greatest relative contribution to the model (Figure 4). Together, the probability of inundation and distance from the channel were chosen nearly half the time (23% and 21%, respectively) in determining the full ensemble model. In total, the first BRT model described 81% of the variability in *P_Dep_{yr}*, and cross-validation of the BRT model (resampling without replacement) showed that the model was moderately predictive (0.58 CV correlation). Valley (*S*, *W_{FP}*, and *IR*) and watershed-scale attributes (*WS_{WET}*, *DA*, *WS_{HSGD}*) described the remaining 32% and 25% of the variability, respectively.

TABLE 4 Spearman rank correlations between plot-scale measurements of sediment mass and phosphorus concentration and environmental variables. Statistically significant relationships ($p < 0.05$) are shown in italics

	Sediment deposition (kg m ⁻²)	P concentration (mg kg ⁻¹)
DA	0.12	-0.13
% Watershed wetland	-0.22	-0.10
% Watershed agriculture	-0.17	0.39
% Watershed HSGD	-0.12	0.41
% Watershed developed	-0.01	0.39
Floodplain width/channel width	-0.02	0.20
Slope	0.18	-0.18
SSP	0.27	-0.28
Distance/channel width	-0.24	0.18
<i>IR</i>	0.03	-0.14
Inundation probability	0.11	0.20

Important thresholds existed in many of the relationships between explanatory variables and *P_Dep_{yr}*. Notably, settings where $S < 0.0015$ and $WS_{WET} > 5\%$ had significantly lower *P_Dep_{yr}*. For floodplains whose *DA* was less than 150 km², *WS_{HSGD}* was greater than 40%, and when *IR* was greater than 1.6, *P_Dep_{yr}* was also smaller.

Phosphorus deposition rates increased with increasing probability of inundation; deposition rates on surfaces inundated regularly (i.e., every 1–2 years) were two to four times greater than those inundated less frequently (i.e., less than every 10 years; Figure 4).

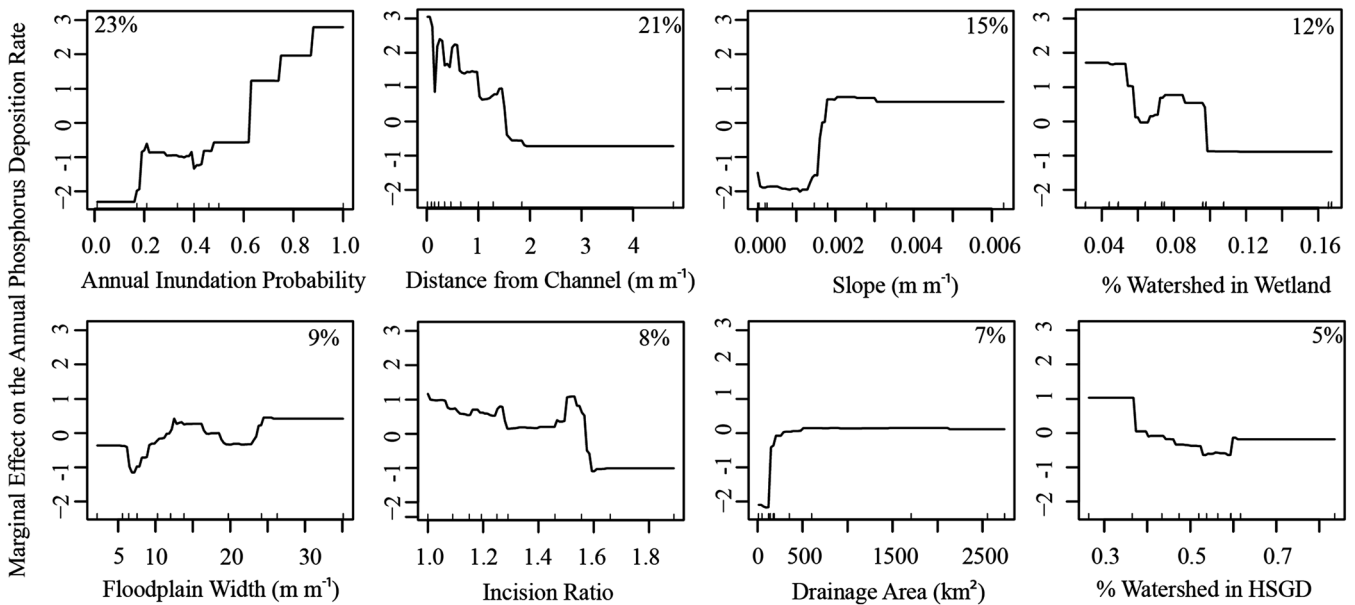


FIGURE 4 Results of boosted regression tree analysis, indicating the relative contribution (%) of physical characteristics (upper corner of each plot) to the total model of annual phosphorus deposition rate ($\text{g P m}^{-2} \text{yr}^{-1}$). Partial dependence plots communicate the effect of each predictor variable after accounting for the average effects of all other variables in the model

Phosphorus deposition rates decreased rapidly with increasing distance from the channel; within one channel width, rates were two to three times greater than they were at two channel widths. Beyond that, the partial dependence plot suggests that deposition rates remain relatively constant and small in magnitude, although very little of our data were collected beyond two channel widths (e.g., 90% of the plots had D values < 2).

$Inun$ had a strong interaction with S , and to a lesser degree with D . The importance of inundation probability on deposition differed in settings where channel gradient was low from those settings that were steeper and depended on the proximity to the stream channel. Even though areas closer to the channel tended to be inundated more frequently than those further away, $Inun$ and D were not correlated ($\rho = -0.12$, $p = 0.18$), likely because of other confounding factors such as variability in vertical connectivity or floodplain topography.

Annual site-scale floodplain phosphorus deposition (P_{DepFP} ; $\text{g m}^{-1} \text{yr}^{-1}$) increased with drainage area, but this relationship differed based on channel slope and depended on valley confinement (Figure 5). In unconfined settings, P_{DepFP} was greater when channel slope was steeper than 0.0015 than for sites where channel slopes were less than 0.0015 (ANOVA, $p = 0.01$). Two sites are located within confined valleys (i.e., $W_{FP} < 4$ channel widths; Vermont Agency of Natural Resources, 2009), and as a result their floodplains are much narrower than the other sites for a given drainage area (Figure 5). Here, P_{DepFP} was much less than would be predicted given their location in the watershed and the slope of the channel.

3.3 | Scenario analysis in two headwater watersheds

The simpler, predictive, BRT model included five variables representative of cross-scale physical characteristics of the watershed, valley, and local setting, as well as the three dimensions of hydrologic

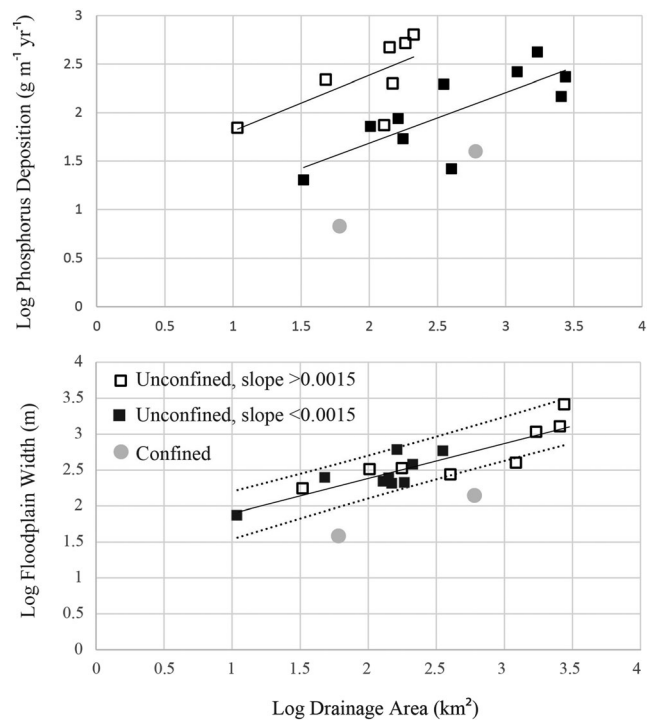


FIGURE 5 Annual site-scale floodplain phosphorus deposition scales to drainage area, but the relationship differs based on channel slope and confinement (top). Floodplain width scales with drainage area for all but two sites that are located in confined settings (floodplain width $< 4 \times$ channel width). Solid lines indicate significant ($p < 0.01$) relationships between log drainage area and log phosphorus deposition (top) and log floodplain width (bottom) with 95% confidence interval (dashed lines)

connectivity (longitudinal (WS_{WET}), vertical (IR), and lateral ($Inun$); Figure 6). Variables were classified into three or four categories, based on apparent breaks in partial dependence plots from the original model (see Figure 4 and Table 5). Because we limited the number of

FIGURE 6 Partial dependence plot summarizing results from boosted regression tree analysis developed to predict P deposition patterns through a watershed

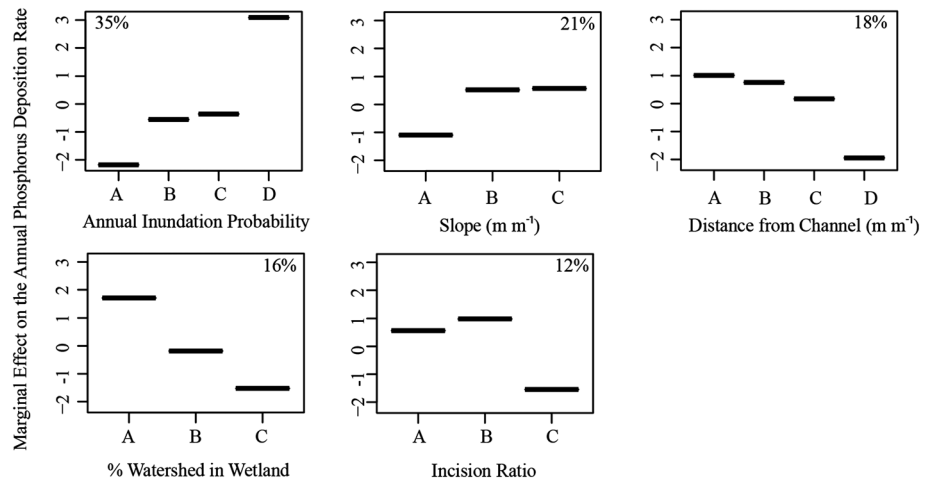


TABLE 5 Categories for classification of variables used in simplified BRT model used to make predictions about deposition patterns for existing and potential conditions in two watersheds

Variable	Class	Value	Description
WS_{WET}	A	<5%	Low storage
	B	5–10%	Moderate storage
	C	>10%	High storage
S	A	<0.001	Low gradient
	B	0.001 to 0.002	Moderate gradient
	C	>0.002	High gradient
IR	A	1.0 to 1.3	Well-connected floodplain
	B	1.3 to 1.6	Moderately-connected floodplain
	C	>1.6	Disconnected floodplain
Dist	A	<0.5 m m ⁻¹	Near-channel region
	B	0.5 to 1.0 m m ⁻¹	
	C	1.0 to 1.5 m m ⁻¹	
	D	>1.5 m m ⁻¹	Distal floodplain
Inun	A	<0.20	Rarely inundated
	B	0.20 to 0.50	Infrequently inundated
	C	0.5	Two-year floodplain
	D	>0.50	Annual floodplain

variables and converted them to categorical variables, the predictive BRT model described less variability (50%) than the full BRT and was moderately predictive (51% of CV).

Application of the predictive model to the Mad River and Black Creek watersheds demonstrated how cross-scale physical characteristics and hydrologic (dis)connectivity influenced floodplain deposition. Existing phosphorus deposition rates ($\text{g P m}^{-1} \text{ yr}^{-1}$) and total mass of phosphorus deposited within the watershed (kg P yr^{-1}) were similar for the Mad River and Black Creek (Table 6). Higher gradient reaches along the Mad River, which are associated with greater floodplain deposition rates were offset by greater vertical (*IR*) and lateral (*Inun*) disconnectivity. Because of the Mad River's generally larger *IR* and lower *Inun* values as compared to Black Creek, the difference in phosphorus deposition rates between existing and potential scenarios was greater; median deposition rates increased 110% on the Mad River from existing to potential and 20% on the Black Creek (Table 6). On a per stream length basis, potential deposition rates were similar between the watersheds because 100% of the Black Creek's stream

length in our study area supports floodplains compared to 61% of the Mad River study area.

4 | DISCUSSION

4.1 | Spatial patterns of floodplain deposition

Event-scale measurements of sediment and phosphorus deposition, collected across large environmental gradients, demonstrate that strong spatial trends exist in floodplain deposition and therefore in the functioning of these landforms. Through a watershed, we would expect total floodplain deposition to scale with drainage area (Magilligan, 1985; Swinnen, Daniëls, et al., 2020), in part because floodplain width determines accommodation space, and floodplain width generally increases along the longitudinal profile of a river. Through the Lake Champlain Basin, we documented changes in deposition that scaled with drainage area, but these trends were

TABLE 6 Watershed and phosphorus deposition characteristics for two test-case watersheds for existing and potential (e.g., full hydrologic connectivity) conditions. Listed values are medians with minimum and maximum in parentheses. Watershed characteristics do not change between the existing and potential scenarios

	Mad River		Black Creek	
	Existing	Potential	Existing	Potential
Watershed characteristics				
Total stream length (DA > 25 km ² ; km)	51		51	
% of stream length with floodplain deposition	61%		100%	
Slope ^a	0.01 (0.0003–0.06)		0.001 (0.0001–0.02)	
% Watershed in wetland	3.7%		9.0%	
Hydrologic connectivity metrics				
Annual probability of inundation	0.19 (0.03–0.50)	0.39 (0.11–0.99)	0.50 (0.10–0.50)	0.55 (0.11–0.76)
Incision ratio	1.6 (1.0–2.8)	1.0	1.3 (1.0–2.0)	1.0
Reach averages				
P deposition rate (g P m ⁻² yr ⁻¹)	2.3 (0–8.0)	4.8 (0–13.9)	2.1 (0.8–6.6)	2.5 (1.2–10.8)
Annual P deposition (g P m ⁻¹ yr ⁻¹)	213 (0–693)	448 (0–1,133)	169 (45–398)	252 (49–521)
Watershed total				
Annual P deposition (g P m ⁻¹ yr ⁻¹)	146	266	226	262
Total annual P deposition (kg P yr ⁻¹)	7478	13,664	11,521	13,325

^aFor all streams within watershed with DA > 25 km².

discontinuous and depended on variations in valley width and slope. Discontinuous downstream changes in valley geometry affect the presence and character of floodplains (Brierley, 2009; Jain et al., 2008; Van Appledorn et al., 2019) and the capacity to store sediment, nutrients, and carbon (Lininger & Wohl, 2019; Swinnen, Daniëls, et al., 2020) and support diverse aquatic and riparian ecosystems (Bellmore & Baxter, 2014; Goebel et al., 2003).

Nanson and Croke (1992) defined floodplain types based on the geomorphic context, framing their classification as the balance between stream power and sediment character. In higher-energy settings, larger quantities of coarser sediment sizes may be moved more efficiently. Our event-scale observations indicate that deposition rates are greater where stream power, and relatedly slope, is moderately large. We found that this threshold in process occurs for channel slopes around 0.001 to 0.002 m m⁻¹ and is consistent with transitions in river character and behavior documented elsewhere, including the shift from low-energy to medium-energy floodplains in the Nanson and Croke Classification, and from sand to gravel bed rivers (Sklar & Dietrich, 1998; Figure 2). In lower-gradient watersheds of the Lake Champlain Basin dominated by glaciolacustrine deposits, the finer-grained deposits sourced from cohesive channel boundaries are associated with smaller depositional thickness (and mass) in adjacent floodplains. Fine-grained streambank sediments (silts, clays) tend to have a greater affinity for phosphorus due to their greater surface area (McDowell et al., 2002), and therefore are generally characterized by greater phosphorus concentrations than coarse-grained sediments in Vermont streambanks (Ishee et al., 2015; Young et al., 2012) consistent with findings from other regions, such as the Chesapeake Bay (Lutgen et al., 2020). Flood-deposited sediments sampled in this study were weakly associated with percent fines (Triantafyllou, 2021), and total phosphorus deposition was strongly associated with deposit thickness, where thicker deposits tend to have coarser grains.

Although variability in deposition through a watershed can be large, local differences through a reach or across a floodplain are often

greater (e.g., Lininger et al., 2018). In our study, local characteristics of water and sediment transport dynamics, including distance to the channel and frequency of inundation, had greater relative influence on the BRT model than valley and watershed characteristics. Most sediment falls out of suspension as water crosses the river–floodplain threshold, resulting in a rapid decrease in deposition with distance from the channel (Middelkoop & Asselman, 1998; Moody et al., 1999). Floodplain areas close to the channel, or which are directly connected to the channel through levee breaches or preferential side channels, consistently experience greater deposition, especially when flooded frequently (Kaase & Kupfer, 2016; Pizzuto et al., 2016; Renshaw et al., 2014). The rate of change of deposition is large with increasing distance from a water and sediment source, or with decreasing activation frequency. We documented a rapid drop in deposition more than one to two channel widths away from the channel bank, and with inundation occurring less frequently than every 1–2 years. A large proportion of the deposition that occurs on floodplains, therefore, occurs within a relatively limited spatial zone and time frame, in areas where the transfer of floodwaters from the river channel to floodplain is relatively efficient. Our data suggest that deposition rates in these highly connected spots are at least two to five times greater than other zones of the floodplain. Actions that limit connectivity within this zone have a disproportionate impact on floodplain deposition.

4.2 | Interactions between natural and anthropogenic factors and opportunities for restoring the natural functioning of floodplains

While the capacity of a floodplain to capture sediment may be determined by its geomorphic setting, human impacts are ubiquitous and imprinted on most watershed rainfall–runoff patterns and sediment transport processes (Noe et al., 2020; Walling, 2009). Land use

conversions or direct channel manipulations, for example, can cause substantial shifts in expected deposition patterns (Swinnen, Broothaerts, et al., 2020) and persist for decades or longer (Hupp et al., 2015; Pizzuto et al., 2016). These disturbances may be described by their enhancement of sediment supplies and nutrient concentrations or by the decrease to river network connectivity longitudinally through a watershed, vertically across the river channel/floodplain interface, and laterally over the floodplain. In our study, we found a positive correlation between phosphorus concentration and percent of upstream land uses in agriculture and development, but no significant correlation to total deposition of sediment or phosphorus. Because of the documented importance of connectivity to deposition, at both the watershed scale (Pringle, 2001) and locally (i.e., Section 4.1), restoration practices that increase connectivity can greatly improve functioning (Bartsch et al., 2022; Covino, 2017; Magilligan et al., 2016; McMillan & Noe, 2017). Developing an understanding of the departure in expected hydrologic connectivity can help to prioritize watershed management efforts that address water quality concerns, flood resiliency, and ecological integrity. This exercise may be complicated, however, because of natural discontinuities and large variability in floodplain inundation thresholds and patterns (Burchsted et al., 2014; Petit & Pauquet, 1998; Pizzuto, 1986).

Watershed management interventions may differ based on the balance between differences in existing and potential deposition, but also in the magnitude of existing deposition. Programs targeting the preservation or conservation of valuable floodplains may target areas where existing deposition rates and connectivity are high. Active restoration may have the biggest impact where differences in existing and potential are greatest. In the scenario analysis, the interactions of the natural setting and hydrologic (dis)connectivity help to highlight how watershed management priorities may play out across the landscape. Floodplains in the Mad River watershed that support deposition (e.g., below slope-DA threshold; Figure 2) have the potential for greater deposition of sediment and phosphorus on a per area basis, suggesting that restoration of individual floodplains may help to further goals associated with sediment and phosphorus attenuation. Yet, because of a greater degree of hydrologic disconnectivity (e.g., higher incision ratios) and less floodplain area in total, the overall storage capacity of the Mad River is less than that of Black Creek, and conservation efforts to achieve downstream water quality benefits may be better directed towards the Black Creek.

Prioritizing watersheds and floodplains for restoration or conservation depends on the management objective and the process-based and temporal frame of reference, and therefore may differ from what is highlighted in our study. Conclusions drawn in this paper are based on a spatially robust dataset of floodplain deposition, measured over a narrow window of time (2 years) and focused exclusively on depositional environments. One of our main conclusions is that floodplains located in moderately steep valleys and in watersheds with low water storage capacity have higher deposition rates. These settings are likely to have flashier hydrology and potentially greater, or at least coarser-grained, sediment loads, but higher energy settings that move large fluxes of material are also highly dynamic. Significant sediment deposition on floodplains is likely to be matched with high rates of bank erosion or resuspension of bed and floodplain sediments (Hupp et al., 2013)—thus, net sediment and nutrient retention at a watershed scale may be less in these settings. Over longer timescales, such as

decades to centuries, lower energy settings may become more important for storage of sediment and nutrients (e.g., Swinnen, Daniëls, et al., 2020). Deposition rates may also shift through time, in response to decadal variability in hydrology, changes in land use patterns, or channel recovery from perturbations such as channelization (Hupp & Bazemore, 1993). Finally, because deposition rates are dependent on the incoming load, evident in the relationships between transport energy (SSP or S) and deposition magnitude, it is important to acknowledge that deposition will shift with a change in sediment or phosphorus loads because of changes in land use patterns, hydrology, or with recovery from past perturbations (e.g., Owens & Walling, 2002).

4.3 | Applicability of observations from regional datasets

The regional dataset described in this paper contributes to an increasing number of studies that document floodplain deposition rates and the functioning of floodplains in the USA (e.g., Knox, 2006; Noe & Hupp, 2005), Europe (e.g., Kronvang et al., 2007; Middelkoop & Asselman, 1998), and elsewhere (e.g., Grenfell et al., 2009; Park & Latrubesse, 2019). We highlight the importance of characteristics such as gradient, watershed water storage, soil characteristics, and hydrologic connectivity that vary significantly among watersheds and from one region to the next, where geologic, climatic, and land use histories differ. Questions remain, however, about the transferability of documented rates and observed spatial patterns from one regional dataset to another.

In Figure 7, we compare our dataset to others in the Chesapeake Bay Region, where significant work has been done in characterizing trends in deposition (Gellis et al., 2008; Noe & Hupp, 2005, 2009; Noe et al., 2019; Schenk et al., 2013). Both regions experienced substantial shifts in land use patterns in the colonial and post-colonial periods, contributing to the storage and subsequent erosion of legacy sediments, and in the contribution of pollutants from agricultural and developed runoff (Kline & Cahoon, 2010; Noe et al., 2020), even though the glacial history of the regions differs substantially (Stewart & MacClintock, 1969; Williams & Reed, 1972). On average, sediment and phosphorus deposition rates in the Lake Champlain and Chesapeake Bay regions are comparable (averaging $2.0 \text{ kg m}^{-2} \text{ yr}^{-1}$ in the LC and $2.3 \text{ kg m}^{-2} \text{ yr}^{-1}$ in the CB [$t[32] = -0.48$, $p = 0.64$], and $1.4 \text{ g P m}^{-2} \text{ yr}^{-1}$ in the LC and $1.1 \text{ g P m}^{-2} \text{ yr}^{-1}$ in the CB [$t[33] = 2.4$, $p = 0.55$]) and have similar landscape-scale trends. Floodplains located in the depositional plains of both regions (Champlain Valley or Coastal Plain) have lower depositional rates than the more upland physiographic province (Green Mountain or Piedmont). When the datasets are combined across regions for sediment deposition, differences in uplands are twice that of depositional plains (average depositional plain = $1.5 \text{ kg m}^{-2} \text{ yr}^{-1}$, $SD = 2.6$, and average upland = $3.1 \text{ kg m}^{-2} \text{ yr}^{-1}$, $SD = 1.5$ [$t[33] = 2.4$, $p = 0.02$]). The transition from upland to lowland provinces in the two regions correspond to a decrease in gradient, and a shift in floodplain type (from medium- to low-energy) and deposition.

At the watershed scale, observations of distinct process domains may be transferrable and help in understanding coarse patterns in expected deposition. Findings from this study may be used outside of

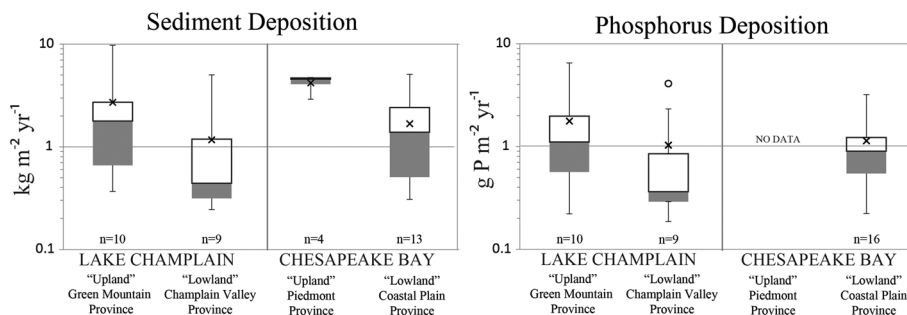


FIGURE 7 Sediment and phosphorus deposition rates in Lake Champlain and Chesapeake Bay regions are, on average, similar. Box plots indicate upper quartile (white shading) and lower quartile (gray shading), as well as sample average (“x”) and minimum and maximum values (whiskers). In both regions, deposition rates are larger in the upland provinces, where channel gradients are steeper than in the lowland provinces. Sediment deposition rates for the Chesapeake Bay are from Gellis et al. (2008), Noe et al. (2019), and Schenk et al. (2013). Phosphorus deposition rates are from McMillan and Noe (2017), Noe and Hupp (2005, 2009), and Noe et al. (2019), and are all located in the Coastal Plain of the Chesapeake Bay. Two of the nine Lake Champlain “lowland” sites are in low-lying physiographic provinces different from the Champlain Valley (Hudson Valley and Valley of Vermont)

the region to rank the potential functioning of floodplains in, for example, a watershed management plan to meet water quality goals. Our work highlights the important consideration of physiographic province, and slope more generally, as a determinant of where sediment and sediment-bound phosphorus deposition may be greater (upland settings, where slopes are moderate), but also the impact of well-connected floodplains on reducing watershed sediment and nutrient fluxes. While some general trends may be extracted from our study, additional empirical studies of this type in other settings will continue to build the place-based context needed to constrain deposition rates for use in more granular-scale planning.

5 | CONCLUSIONS

This study developed a dataset on the functioning of floodplains in the Lake Champlain Basin in Vermont, the first dataset of its kind in the region. Average rates were comparable with the nearby Chesapeake Bay region, averaging approximately $1.3 \text{ kg m}^{-2} \text{ yr}^{-1}$ of sediment and $2.1 \text{ g P m}^{-2} \text{ yr}^{-1}$ of phosphorus. Floodplains in the Lake Champlain Basin can capture as much as $22 \text{ kg m}^{-2} \text{ yr}^{-1}$ of sediment or $42 \text{ g P m}^{-2} \text{ yr}^{-1}$ in areas of the floodplain that are close to the river and are frequently flooded, and where channel slopes in valleys that support floodplains are moderately steep ($\sim 0.002 \text{ m m}^{-1}$). In contrast, deposition rates can range as low as $0.1 \text{ kg m}^{-2} \text{ yr}^{-1}$ of sediment or $0.1 \text{ g m}^{-2} \text{ yr}^{-1}$ of phosphorus. Such low rates may be associated with increased distance from the channel, or lower inundation frequency, and where particle sizes are smaller because of less transport energy and/or the nature and genesis of channel boundary materials.

The results of this work highlight how the watershed and valley setting, and the frequency with which the floodplain is inundated, are correlated with variability in sediment and phosphorus deposition on floodplains. By developing a novel dataset of event-scale measurements collected across large environmental gradients that account for the frequency of depositional events, we were able to analyze spatial patterns in floodplain deposition in a robust way. A cross-scale perspective that merged local and watershed assessments highlighted spatial patterns in an integrated way. Our findings suggest that variability through a watershed, or across a region, can be large, but that

greater variability exists locally across a floodplain, because of differences in the proximity to water and sediment sources, and frequency of inundation.

There is growing interest in restoring the capacity of the natural infrastructure of a watershed or using nature-based solutions to meet water quality goals, especially when these actions may have additional co-benefits of increasing flood resiliency for communities and improving the quality of riparian habitats. The characterization of spatial patterns and quantification of deposition rates will help to highlight the importance of conserving functioning floodplains as well as reconnecting floodplains, especially in settings where the natural capacity to capture sediment and nutrients is great. Because of the interrelated nature of depositional and erosional processes and the complex dynamics of phosphorus movement through a watershed, future work should focus on a more holistic characterization of floodplain retention, to better inform sediment and nutrient management. Such perspectives would account for not only floodplain deposition, as our study has, but also bank erosion, sediment and nutrient resuspension, and nutrient transformations that contribute to the net capture and storage.

ACKNOWLEDGMENTS

This study was funded by a technical grant from the Lake Champlain Basin Program and the Vermont Department of Environmental Conservation. Additional support was provided by the University of Vermont Gund Institute on the Environment, The Nature Conservancy Vermont, and the National Science Foundation under VT EPSCoR Grant. We would like to thank Dan Needham for help in the lab, and Adrian Wiegman, Shayne Jaquith, Allaire Diamond, Sumana Serchan, and Staci Pomeroy for assistance with site identification and permissions.

AUTHOR CONTRIBUTIONS

Conceptualization: Rebecca M. Diehl, Beverley C. Wemple. *Funding acquisition:* Rebecca M. Diehl, Beverley C. Wemple, Kristen L. Underwood. *Methodology:* Rebecca M. Diehl, Kristen L. Underwood, Beverley C. Wemple, Don S. Ross. *Investigation:* RMD, SPT, SD. *Resources:* SPT, SD, DSR. *Software:* N/A. *Supervision:* Rebecca M. Diehl, Beverley C. Wemple. *Writing:* Rebecca M. Diehl. *Reviewing and editing:* Kristen L. Underwood, Beverley C. Wemple.

DATA AVAILABILITY STATEMENT

The datasets generated and analyzed during the current study are available from the corresponding author on reasonable request.

ORCID

Rebecca M. Diehl  <https://orcid.org/0000-0001-9414-4045>

Beverley C. Wemple  <https://orcid.org/0000-0002-3155-9099>

REFERENCES

- Bartsch, L.A., Kreiling, R., Gruhn, L.R., Garrett, J.D., Richardson, W.B. & Nalley, G.M. (2022) Sediment and Nutrient Retention on a Reconnected Floodplain of an Upper Mississippi River Tributary, 2013–2018 [online] Available from: <https://doi.org/10.3133/sir20225030>
- Beechie, T.J., Pollock, M.M. & Baker, S. (2008) Channel incision, evolution and potential recovery in the Walla Walla and Tucannon River basins, northwestern USA. *Earth Surface Processes and Landforms*, 33(5), 784–800. Available from: <https://doi.org/10.1002/esp.1578>
- Bellmore, J.R. & Baxter, C.V. (2014) Effects of geomorphic process domains on river ecosystems: A comparison of floodplain and confined valley segments. *River Research and Applications*, 30(5), 617–630. Available from: <https://doi.org/10.1002/rra.2672>
- Bergen, K., Johnson, P., de Hoop, M. & Beroza, G. (2019) Machine learning for data-driven discovery in solid Earth geoscience. *Science*, 363(6433), eaau0323. Available from: <https://doi.org/10.1126/science.aau0323>
- Brierley, G.J. (2009) Landscape memory: the imprint of the past on contemporary landscape forms and processes. *Area*, 42(1), 76–85. Available from: <https://doi.org/10.1111/j.1475-4762.2009.00900.x>
- Brunet, R. & Astin, K.B. (1998) Variation in phosphorus flux during a hydrological season: The River Adour. *Water Research*, 32(3), 547–558. Available from: [https://doi.org/10.1016/S0043-1354\(97\)00317-5](https://doi.org/10.1016/S0043-1354(97)00317-5)
- Burchsted, D., Daniels, M. & Wohl, E.E. (2014) Introduction to the special issue on discontinuity of fluvial systems. *Geomorphology*, 205, 1–4. Available from: <https://doi.org/10.1016/j.geomorph.2013.04.004>
- Church, M. (2002) Geomorphic thresholds in riverine landscapes. *Freshwater Biology*, 47(4), 541–557. Available from: <https://doi.org/10.1046/j.1365-2427.2002.00919.x>
- Collins, M.J., Kirk, J.P., Pettit, J., DeGaetano, A.T., McCown, M.S., Peterson, T.C. et al. (2014) Annual floods in New England (USA) and Atlantic Canada: synoptic climatology and generating mechanisms. *Physical Geography*, 35(3), 195–219. Available from: <https://doi.org/10.1080/02723646.2014.888510>
- Covino, T. (2017) Hydrologic connectivity as a framework for understanding biogeochemical flux through watersheds and along fluvial networks. *Geomorphology*, 277, 133–144. Available from: <https://doi.org/10.1016/j.geomorph.2016.09.030>
- De Vente, J., Poesen, J. & Verstraeten, G. (2007) The sediment delivery problem revisited. *Progress in Physical Geography*, 31(2), 155–178. Available from: <https://doi.org/10.1177/0309133307076485>
- Diehl, R.M., Gourevitch, J.D., Drago, S. & Wemple, B.C. (2021) Improving flood hazard datasets using a low-complexity, probabilistic floodplain mapping approach. *PLoS ONE*, 1–20(3), e0248683. Available from: <https://doi.org/10.1371/journal.pone.0248683>
- Diehl, R.M., Wemple, B.C., Underwood, K.L. & Ross, D. (2021) Evaluating floodplain potential for sediment and phosphorus deposition: Development of a framework to assist in Lake Champlain Basin planning.
- Elith, J., Leathwick, J.R. & Hastie, T. (2008) A working guide to boosted regression trees. *Journal of Animal Ecology*, 77(4), 802–813. Available from: <https://doi.org/10.1111/j.1365-2656.2008.01390.x>
- Environmental Protection Agency. (2016) *Phosphorus TMDLs for Vermont Segments of Lake Champlain*. New England, MA: US Environmental Protection Agency Region 1.
- Gellis, A.C., Hupp, C.R., Pavich, M.J., Landwehr, J.M., Banks, W.S.L., Hubbard, B.E. et al. (2008) Sources, transport, and storage of sediment in the Chesapeake Bay Watershed: US Geological Survey Scientific Investigations Report 2008–5186.
- Goebel, P.C., Palik, B.J. & Pregitzer, K.S. (2003) Plant diversity contributions of riparian areas in watersheds of the northern Lake States, USA. *Ecological Applications*, 13(6), 1595–1609. Available from: <https://doi.org/10.1890/01-5314>
- Gordon, B.A., Dorothy, O. & Lenhart, C.F. (2020) Nutrient retention in ecologically functional floodplains: A review. *Water (Switzerland)*, 12(10), 15–17. Available from: <https://doi.org/10.3390/w12102762>
- Gourevitch, J.D., Singh, N.K., Minot, J., Raub, K.B., Wemple, B.C., Ricketts, T.H. et al. (2020) Spatial targeting of floodplain restoration to equitably mitigate flood risk. *Global Environmental Change*, 61, 102050. Available from: <https://doi.org/10.1016/j.gloenvcha.2020.102050>
- Grenfell, S.E., Ellery, W.N. & Grenfell, M.C. (2009) Geomorphology and dynamics of the Mfolozi River floodplain, KwaZulu-Natal, South Africa. *Geomorphology*, 107(3–4), 226–240. Available from: <https://doi.org/10.1016/j.geomorph.2008.12.011>
- Hijmans, R., Phillips, J., Leathwick, J.R. & Elith, J. (2015) *dismo: Species distribution modeling, R package version 1.0–12* (The R Foundation for Statistical Computing). Vienna: The R Foundation for Statistical Computing.
- Hupp, C.R. & Bazemore, D.E. (1993) Temporal and spatial patterns of wetland sedimentation, West Tennessee. *Journal of Hydrology*, 141(1–4), 179–196. Available from: [https://doi.org/10.1016/0022-1694\(93\)90049-F](https://doi.org/10.1016/0022-1694(93)90049-F)
- Hupp, C.R., Demas, C.R., Kroes, D.E., Day, R.H. & Doyle, T.W. (2008) Recent sedimentation patterns within the central Atchafalaya Basin, Louisiana. *Wetlands*, 28(1), 125–140. Available from: <https://doi.org/10.1672/06-132.1>
- Hupp, C.R., Noe, G.B., Schenk, E.R. & Bentham, A.J. (2013) Recent and historic sediment dynamics along Difficult Run, a suburban Virginia Piedmont stream. *Geomorphology*, 180–181, 156–169. Available from: <https://doi.org/10.1016/j.geomorph.2012.10.007>
- Hupp, C.R., Schenk, E.R., Kroes, D.E., Willard, D.A., Townsend, P.A. & Peet, R.K. (2015) Geomorphology Patterns of floodplain sediment deposition along the regulated lower Roanoke River, North Carolina: Annual, decadal, centennial scales. *Geomorphology*, 228, 666–680. Available from: <https://doi.org/10.1016/j.geomorph.2014.10.023>
- Ishee, E.R., Ross, D.S., Garvey, K.M., Bourgault, R.R. & Ford, C.R. (2015) Phosphorus Characterization and Contribution from Eroding Streambank Soils of Vermont's Lake Champlain Basin. *Journal of Environmental Quality*, 44(6), 1745–1753. Available from: <https://doi.org/10.2134/jeq2015.02.0108> [online] Available from: <https://dl.sciencesocieties.org/publications/jeq/abstracts/44/6/1745>
- Isles, P.D.F., Giles, C.D., Gearhart, T.A., Xu, Y., Druschel, G.K. & Schroth, A. (2015) Dynamic internal drivers of a historically severe cyanobacteria bloom in Lake Champlain revealed through comprehensive monitoring. *Journal of Great Lakes Research*, 41(3), 818–829. Available from: <https://doi.org/10.1016/j.jglr.2015.06.006>
- Jain, V., Fryirs, K. & Brierley, G. (2008) Where do floodplains begin? The role of total stream power and longitudinal profile form on floodplain initiation processes. *Bulletin of the Geological Society of America*, 120(1–2), 127–141. Available from: <https://doi.org/10.1130/B26092.1>
- Johnson, T.A.N., Kaushal, S.S., Mayer, P.M., Smith, R.M. & Sivirichi, G.M. (2016) Nutrient Retention in Restored Streams and Rivers: A Global Review and Synthesis. *Water*, 8(4), 1–29, 116. Available from: <https://doi.org/10.3390/w8040116>
- Kaase, C.T. & Kupfer, J.A. (2016) Sedimentation patterns across a Coastal Plain floodplain: The importance of hydrogeomorphic influences and cross-floodplain connectivity. *Geomorphology*, 269, 43–55. Available from: <https://doi.org/10.1016/j.geomorph.2016.06.020>
- Kleiss, B.A. (1996) Sediment retention in a bottomland hardwood wetland in Eastern Arkansas. *Wetlands*, 16(3), 321–333. Available from: <https://doi.org/10.1007/BF03161333>
- Kline, M., Alexander, C., Jaquith, S., Pomeroy, S. & Springston, G. (2009) *Vermont ANR Stream Geomorphic Assessment Protocol Handbooks*. Waterbury, Vermont: Vermont Agency of Natural Resources.
- Kline, M. & Cahoon, B. (2010) Protecting river corridors in Vermont. *Journal of the American Water Resources Association*, 46(2), 227–236. Available from: <https://doi.org/10.1111/j.1752-1688.2010.00417.x>

- Knox, J.C. (2006) Floodplain sedimentation in the Upper Mississippi Valley: Natural versus human accelerated. *Geomorphology*, 79(3-4), 286-310. Available from: <https://doi.org/10.1016/j.geomorph.2006.06.031>
- Kronvang, B., Andersen, I.K., Hoffmann, C.C., Pedersen, M.L., Ovesen, N. B. & Andersen, H.E. (2007) Water exchange and deposition of sediment and phosphorus during inundation of natural and restored lowland floodplains. *Water, Air, and Soil Pollution*, 181(1-4), 115-121. Available from: <https://doi.org/10.1007/s11270-006-9283-y>
- Langendoen, E. J., Simon, A., Klimetz, L., Bankhead, N., & Ursic, M. E. (2012) Quantifying Sediment Loadings from Streambank Erosion in Selected Agricultural Watersheds Draining to Lake Champlain.
- Lininger, K.B. & Wohl, E. (2019) Floodplain dynamics in North American permafrost regions under a warming climate and implications for organic carbon stocks: A review and synthesis. *Earth-Science Reviews*, 193, 24-44. Available from: <https://doi.org/10.1016/j.EARSCIREV.2019.02.024>
- Lininger, K.B., Wohl, E. & Rose, J.R. (2018) Geomorphic Controls on Floodplain Soil Organic Carbon in the Yukon Flats, Interior Alaska, From Reach to River Basin Scales. *Water Resources Research*, 54(3), 1934-1951. Available from: <https://doi.org/10.1002/2017WR022042>
- Lutgen, A., Jiang, G., Sienkiewicz, N., Mattern, K., Kan, J. & Inamadar, S. (2020) Nutrients and heavy metals in legacy sediments: Concentrations, comparisons with upland soils, and implications for water quality. *Journal of the American Water Resources Association*, 56(4), 669-691. Available from: <https://doi.org/10.1111/1752-1688.12842>
- Magilligan, F.J. (1985) Historical Floodplain Sedimentation in the Galena River Basin, Wisconsin and Illinois. *Annals of the Association of American Geographers*, 75(4), 583-594. Available from: <https://doi.org/10.1111/j.1467-8306.1985.tb00095.x>
- Magilligan, F.J., Graber, B.E., Nislow, K.H., Chipman, J.W., Sneddon, C.S. & Fox, C.A. (2016) River restoration by dam removal: Enhancing connectivity at watershed scales. *Elementa*, 2016, 1-14. Available from: <https://doi.org/10.12952/journal.elementa.000108>
- McCluney, K.E., Poff, N.L., Palmer, M.A., Thorp, J.H., Poole, G.C., Williams, B.S. et al. (2014) Riverine macrosystems ecology: Sensitivity, resistance, and resilience of whole river basins with human alterations. *Frontiers in Ecology and the Environment*, 12(1), 48-58. Available from: <https://doi.org/10.1890/120367>
- McDowell, R.W., Sharpley, A.N. & Chalmers, A.T. (2002) Land use and flow regime effects on phosphorus chemical dynamics in the fluvial sediment of the Winooski River, Vermont. *Ecological Engineering*, 18(4), 477-487. Available from: [https://doi.org/10.1016/S0925-8574\(01\)00108-2](https://doi.org/10.1016/S0925-8574(01)00108-2)
- McMillan, S.K. & Noe, G.B. (2017) Increasing floodplain connectivity through urban stream restoration increases nutrient and sediment retention. *Ecological Engineering*, 108, 284-295. Available from: <https://doi.org/10.1016/j.ecoleng.2017.08.006>
- Medalie, L., Hirsch, R.M. & Arch, S.A. (2012) Use of flow-normalization to evaluate nutrient concentration and flux changes in Lake Champlain tributaries, 1990-2009. *Journal of Great Lakes Research*, 38, 58-67. Available from: <https://doi.org/10.1016/j.jglr.2011.10.002>
- Middelkoop, H. & Asselman, N.E.M. (1998) Spatial variability of floodplain sedimentation at the event scale in the Rhine-Meuse Delta, the Netherlands. *Earth Surface Processes and Landforms*, 23(6), 561-573. Available from: [https://doi.org/10.1002/\(SICI\)1096-9837\(199806\)23:6<561::AID-ESP870>3.0.CO;2-5](https://doi.org/10.1002/(SICI)1096-9837(199806)23:6<561::AID-ESP870>3.0.CO;2-5)
- Moody, J.A., Pizzuto, J.E. & Meade, R.H. (1999) Ontogeny of a flood plain. *Geological Society of America Bulletin*, 111(2), 291-303. Available from: [https://doi.org/10.1130/0016-7606\(1999\)111<0291:OOAFP>2.3.CO;2](https://doi.org/10.1130/0016-7606(1999)111<0291:OOAFP>2.3.CO;2)
- Nanson, G.C. & Croke, J.C. (1992) A Genetic Classification of Floodplains. *Geomorphology*, 4, 459-486.
- NOAA National Weather Service. (2021a) Advanced Hydrologic Prediction Service, Multi-sensor precipitation estimates. Available at: <https://water.weather.gov/precip/download.php> [Accessed 15 October 2021].
- NOAA National Weather Service. (2021b) National Operational Hydrologic Remote Sensing Center Archived Datasets, SNOW Data Assimilation System. Available at: https://www.nohrsc.noaa.gov/archived_data/ [Accessed 15 October 2021].
- Noe, G.B., Boomer, K., Gillespie, J.L., Hupp, C.R., Martin-Alciati, M., Floro, K. et al. (2019) The effects of restored hydrologic connectivity on floodplain trapping vs. release of phosphorus, nitrogen, and sediment along the Pocomoke River, Maryland USA. *Ecological Engineering*, 138, 334-352. Available from: <https://doi.org/10.1016/j.ecoleng.2019.08.002>
- Noe, G.B., Cashman, M.J., Skalak, K., Gellis, A., Hopkins, K.G., Moyer, D. et al. (2020) Sediment dynamics and implications for management: State of the science from long-term research in the Chesapeake Bay watershed, USA. *Wiley Interdisciplinary Reviews Water*, 7(4), 1-28. Available from: <https://doi.org/10.1002/wat2.1454>
- Noe, G.B., Hopkins, K.G., Claggett, P.R., Schenk, E.R., Metes, M.J., Ahmed, L. et al. (2022) Streambank and floodplain geomorphic change and contribution to watershed material budgets. *Environmental Research Letters*, 17(6), 064015. Available from: <https://doi.org/10.1088/1748-9326/ac6e47>
- Noe, G.B. & Hupp, C.R. (2005) Carbon, nitrogen, and phosphorus accumulation in floodplains of Atlantic Coastal Plain rivers, USA. *Ecological Applications*, 15(4), 1178-1190. Available from: <https://doi.org/10.1890/04-1677>
- Noe, G.B. & Hupp, C.R. (2009) Retention of riverine sediment and nutrient loads by coastal plain floodplains. *Ecosystems*, 12(5), 728-746. Available from: <https://doi.org/10.1007/s10021-009-9253-5>
- Olde Venterink, H., Vermaat, J.E., Pronk, M., Wiegman, F., van der Lee, G. E.M., van den Hoorn, M.W. et al. (2006) Importance of sediment deposition and denitrification for nutrient retention in floodplain wetlands. *Applied Vegetation Science*, 9(2), 163. Available from: [https://doi.org/10.1658/1402-2001\(2006\)9\[163:iosdad\]2.0.co;2](https://doi.org/10.1658/1402-2001(2006)9[163:iosdad]2.0.co;2)
- Olsen, A.S., Zhou, Q., Linde, J.J. & Arnbjerg-Nielsen, K. (2015) Comparing Methods of Calculating Expected Annual Damage in Urban Pluvial Flood Risk Assessments. *Water*, 7, 255-270. Available from: <https://doi.org/10.3390/w7010255> [online] Available from: www.mdpi.com/journal/waterArticle
- Olson, S.A. (2014) Estimation of flood discharges at selected annual exceedance probabilities for unregulated, rural streams in Vermont.
- Opperman, J.J., Galloway, G.E., Fargione, J., Mount, J.F., Richter, B.D. & Secchi, S. (2009) Sustainable floodplains through large-scale reconnection to rivers. *Science*, 326(5959), 1487-1489. Available from: <https://doi.org/10.1126/science.1178256>
- Opperman, J.J., Luster, R., McKenney, B.A., Roberts, M. & Meadows, A.W. (2010) Ecologically Functional Floodplains: Connectivity, Flow Regime, and Scale. *Journal of the American Water Resources Association*, 46(2), 211-226. Available from: <https://doi.org/10.1111/j.1752-1688.2010.00426.x>
- Owens, P.N. & Walling, D.E. (2002) Changes in sediment sources and floodplain deposition rates in the catchment of the River Tweed, Scotland, over the last 100 years: The impact of climate and land use change. *Earth Surface Processes A N D Landforms*, 423(4), 403-423. Available from: <https://doi.org/10.1002/esp.327>
- Palaseanu-lovejoy, M., Danielson, J., Thatcher, C., Foxgrover, A. & Barnard, P. (2016) Automatic Delineation of Seacliff Limits using Lidar-derived High-resolution DEMs in Southern California. *Journal of Coastal Research*, 76, 162-173. Available from: <https://doi.org/10.2112/SI76-014>
- Park, E. & Latrubesse, E.M. (2019) A geomorphological assessment of wash-load sediment fluxes and floodplain sediment sinks along the lower Amazon River. *Geology*, 47(5), 403-406. Available from: <https://doi.org/10.1130/G45769.1>
- Petit, F. & Pauquet, A. (1998) Bankfull Discharge Recurrence Interval in Gravel-bed Rivers. *Earth Surface Processes and Landforms*, 22, 685-693.
- Phillips, J.D. (2003) Sources of nonlinearity and complexity in geomorphic systems. *Progress in Physical Geography*, 27(1), 1-23. Available from: <https://doi.org/10.1191/0309133303pp340ra>
- Pittman, S.J., Costa, B.M. & Battista, T.A. (2009) Using Lidar Bathymetry and Boosted Regression Trees to Predict the Diversity and Abundance of Fish and Corals. *Journal of Coastal Research*, 25, 27-38. Available from: <https://doi.org/10.2112/SI53-004.1>

- Pizzuto, J. (1986) Flow variability and the bankfull depth of sand-bed streams of the American midwest. *Earth Surface Processes and Landforms*, 11(4), 441–450. Available from: <https://doi.org/10.1002/esp.3290110409>
- Pizzuto, J., Skalak, K., Pearson, A. & Benthem, A. (2016) *Active overbank deposition during the last century*. South River, Virginia: Geomorphology [10.1016/j.geomorph.2016.01.006](https://doi.org/10.1016/j.geomorph.2016.01.006).
- Pizzuto, J.E., Moody, J.A. & Meade, R.H. (2008) Anatomy and dynamics of a floodplain, Powder River, Montana, USA. *Journal of Sedimentary Research*, 78(1), 16–28. Available from: <https://doi.org/10.2110/jsr.2008.005>
- Pringle, C.M. (2001) Hydrologic connectivity and the management of biological reserves: A global perspective. *Ecological Applications*, 11(4), 981–998. Available from: [https://doi.org/10.1890/1051-0761\(2001\)011\[0981:HCATMO\]2.0.CO;2](https://doi.org/10.1890/1051-0761(2001)011[0981:HCATMO]2.0.CO;2)
- Randall, A. D. (1996) Mean annual runoff, precipitation, and evapotranspiration in the glaciated northeastern United States, 1951–1980 (U.S. Geol. Surv. Open File Rep. 96–395). Washington, D.C.: U.S. Geological Survey.
- Renshaw, C.E., Abengoza, K., Magilligan, F.J., Dade, W.B. & Landis, J.D. (2014) Impact of flow regulation on near-channel floodplain sedimentation. *Geomorphology*, 205, 120–127. Available from: <https://doi.org/10.1016/j.geomorph.2013.03.009>
- Schenk, E.R., Hupp, C.R., Gellis, A. & Noe, G. (2013) Developing a new stream metric for comparing stream function using a bank-floodplain sediment budget: A case study of three Piedmont streams. *Earth Surface Processes and Landforms*, 38(8), 771–784. Available from: <https://doi.org/10.1002/esp.3314>
- Schumm, S. (1999) Causes and controls of channel incision. In: *Incised River Channels, Processes, Forms, Engineering and Management*. Chichester: John Wiley and Sons Ltd, pp. 19–33.
- Shanley, J.B. & Denner, J.C. (1999) The Hydrology of the Lake Champlain Basin. *Lake Champlain in Transition: From Research Toward Restoration*, 1, 41–66.
- Sklar, L.S. & Dietrich, W.E. (1998) River longitudinal profiles and bedrock incision models: Stream power and the influence of sediment supply. *Geophysical Monograph- American Geophysical Union*, 107, 237–260.
- Smeltzer, E., Shambaugh, A.D. & Stangel, P. (2012) Environmental change in Lake Champlain revealed by long-term monitoring. *Journal of Great Lakes Research*, 38, 6–18. Available from: <https://doi.org/10.1016/j.jglr.2012.01.002>
- Soranno, P.A., Cheruvilil, K.S., Bissell, E.G., Bremigan, M.T., Downing, J.A., Fergus, C.E. et al. (2014) Cross-scale interactions: Quantifying multi-scaled cause-effect relationships in macrosystems. *Frontiers in Ecology and the Environment*, 12(1), 65–73. Available from: <https://doi.org/10.1890/120366>
- Stanford, J.A., Ward, J.V., Liss, W.J., Frissell, C.A., Williams, R.N., Lichatowich, J.A. et al. (1996) A general protocol for restoration of regulated rivers. *Regulated Rivers: Research and Management*, 12(4–5), 391–413. Available from: [https://doi.org/10.1002/\(sici\)1099-1646\(199607\)12:4/5<391::aid-rr436>3.0.co;2-4](https://doi.org/10.1002/(sici)1099-1646(199607)12:4/5<391::aid-rr436>3.0.co;2-4)
- Steiger, J. & Gurnell, A.M. (2003) Spatial hydrogeomorphological influences on sediment and nutrient deposition in riparian zones: observations from the Garonne River, France. *Geomorphology*, 49(1–2), 1–23. Available from: [https://doi.org/10.1016/S0169-555X\(02\)00144-7](https://doi.org/10.1016/S0169-555X(02)00144-7)
- Stewart, D.P. & MacClintock, P. (1969) *The surficial geology and pleistocene history of Vermont (Bulletin No. 31)*. Montpelier, VT: Vermont Geological Survey.
- Swanson, K.M., Watson, E., Aalto, R., Lauer, J.W., Bera, M.T., Marshall, A. et al. (2008) Sediment load and floodplain deposition rates: Comparison of the Fly and Strickland rivers, Papua New Guinea. *Journal of Geophysical Research - Earth Surface*, 113(F1), 2–17. Available from: <https://doi.org/10.1029/2006JF000623>
- Swinnen, W., Broothaerts, N., Hoevers, R. & Verstraeten, G. (2020) Anthropogenic legacy effects control sediment and organic carbon storage in temperate river floodplains. *Catena*, 195, 104897. Available from: <https://doi.org/10.1016/j.catena.2020.104897>
- Swinnen, W., Daniëls, T., Maurer, E., Broothaerts, N. & Verstraeten, G. (2020) Geomorphic controls on floodplain sediment and soil organic carbon storage in a Scottish mountain river. *Earth Surface Processes and Landforms*, 45(1), 207–223. Available from: <https://doi.org/10.1002/esp.4729>
- Temmerman, S., Bouma, T.J., Govers, G., Wang, Z.B., De Vries, M.B. & Herman, P.M.J. (2005) Impact of vegetation on flow routing and sedimentation patterns: Three-dimensional modeling for a tidal marsh. *Journal of Geophysical Research - Earth Surface*, 110(F4), n/a. Available from: <https://doi.org/10.1029/2005JF000301>
- Tockner, K., Pennetzdorfer, D., Reiner, N., Schiemer, F. & Ward, J.V. (1999) Hydrological connectivity, and the exchange of organic matter and nutrients in a dynamic river-floodplain system (Danube, Austria). *Freshwater Biology*, 41(3), 521–535. Available from: <https://doi.org/10.1046/j.1365-2427.1999.00399.x>
- Triantafillou, S. (2021) The role of geomorphic variability on floodplain function: an analysis of sediment and phosphorus deposition, University of Vermont College of Arts and Sciences College Honors Thesis. Available at <https://scholarworks.uvm.edu/>
- Tschikof, M., Gericke, A., Venohr, M., Weigelhofer, G., Bondar-Kunze, E., Kaden, U.S. et al. (2022) The potential of large floodplains to remove nitrate in river basins- The Danube case. *Science of the Total Environment*, 843, 156879. Available from: <https://doi.org/10.1016/j.scitotenv.2022.156879>
- Underwood, K.L., Rizzo, D.M., Dewoolkar, M.M. & Kline, M. (2021) Analysis of reach-scale sediment process domains in glacially-conditioned catchments using self-organizing maps. *Geomorphology*, 382, 107684. Available from: <https://doi.org/10.1016/j.geomorph.2021.107684>
- Underwood, K.L., Rizzo, D.M., Schroth, A.W. & Dewoolkar, M.M. (2017) Evaluating spatial variability in sediment and phosphorus concentration-discharge relationships using Bayesian inference and self-organizing maps. *Water Resources Research*, 53(12), 293–316. Available from: <https://doi.org/10.1002/2017WR021353>
- Van Appledorn, M., Baker, M.E. & Miller, A.J. (2019) River-valley morphology, basin size, and flow-event magnitude interact to produce wide variation in flooding dynamics. *Ecosphere*, 10(1), e02546. Available from: <https://doi.org/10.1002/ecs2.2546>
- Vermont Agency of Natural Resources. (2009) Vermont Stream Geomorphic Assessment Phase 2 Handbook. Available at: <https://dec.vermont.gov/watershed/rivers/river-corridor-and-floodplain-protection/geomorphic-assessment>
- Vermont Agency of Natural Resources. (2021) Stream Geomorphic Assessment Data Management System. Available at: <https://anweb.vt.gov/DEC/SGA/Default.aspx> [Accessed 1 June 2021].
- Vermont Center for Geographic Information. (2018) Vermont land cover data. Available at: <https://geodata.vermont.gov/pages/land-cover> [Accessed 15 September 2018]
- Vermont Center for Geographic Information. (2019) State of Vermont Lidar-Derived Elevation Products. Available at: <https://geodata.vermont.gov/pages/elevation#services> [Accessed 15 January 2019]
- Vidon, P., Karwan, D.L., Andres, A.S., Inamdar, S., Kaushal, S., Morrison, J. et al. (2018) In the path of the Hurricane: impact of Hurricane Irene and Tropical Storm Lee on watershed hydrology and biogeochemistry from North Carolina to Maine, USA. *Biogeochemistry*, 141(3), 351–364. Available from: <https://doi.org/10.1007/s10533-018-0423-4>
- Walling, D.E. (2009) *The Impact of Global Change on Erosion and Sediment Transport by Rivers*. Paris: UNESCO.
- Walling, D.E. & He, Q. (1998) The spatial variability of overbank sedimentation on river floodplains. *Geomorphology*, 24(2–3), 209–223. Available from: [https://doi.org/10.1016/S0169-555X\(98\)00017-8](https://doi.org/10.1016/S0169-555X(98)00017-8)
- Ward, J.V. (1989) The Four-Dimensional Nature of Lotic Ecosystems. *Journal of the North American Benthological Society*, 8(1), 2–8. Available from: <https://doi.org/10.2307/1467397>
- Ward, J.V., Tockner, K. & Schiemer, F. (1999) Biodiversity of floodplain river ecosystems: ecotones and connectivity. *Regulated Rivers: Research & Management*, 15(1–3), 125–139. Available from: [https://doi.org/10.1002/\(SICI\)1099-1646\(199901/06\)15:1/3<125::AID-RRR523>3.0.CO;2-E](https://doi.org/10.1002/(SICI)1099-1646(199901/06)15:1/3<125::AID-RRR523>3.0.CO;2-E)
- Williams, K.F. & Reed, L. (1972) Appraisal of Stream Sedimentation in the Susquehanna River Basin.

- Wohl, E. (2021) An Integrative Conceptualization of Floodplain Storage. *Reviews of Geophysics*, 59(2), e2020RG000724. Available from: <https://doi.org/10.1029/2020rg000724>
- Wohl, E., Bledsoe, B.P., Jacobson, R.B., Poff, N.L., Rathburn, S.L., Walters, D.M. et al. (2015) The natural sediment regime in rivers: Broadening the foundation for ecosystem management. *Bioscience*, 65(4), 358–371. Available from: <https://doi.org/10.1093/biosci/biv002>
- Wohl, E., Brierley, G., Cadol, D., Coulthard, T.J., Covino, T., Fryirs, K.A. et al. (2019) Connectivity as an emergent property of geomorphic systems. *Earth Surface Processes and Landforms*, 44(1), 4–26. Available from: <https://doi.org/10.1002/esp.4434>
- Wohl, E., Lininger, K.B. & Scott, D.N. (2018) River beads as a conceptual framework for building carbon storage and resilience to extreme climate events into river management. *Biogeochemistry*, 141(3), 365–383. Available from: <https://doi.org/10.1007/s10533-017-0397-7>
- Young, E.O., Ross, D.S., Alves, C. & Villars, T. (2012) Soil and landscape influences on native riparian phosphorus availability in three Lake Champlain Basin stream corridors. *Journal of Soil and Water Conservation*, 67(1), 1–7. Available from: <https://doi.org/10.2489/jswc.67.1.1>

SUPPORTING INFORMATION

Additional supporting information can be found online in the Supporting Information section at the end of this article.

How to cite this article: Diehl, R.M., Underwood, K.L., Triantafyllou, S.P., Ross, D.S., Drago, S. & Wemple, B.C. (2023) Multi-scale drivers of spatial patterns in floodplain sediment and phosphorus deposition. *Earth Surface Processes and Landforms*, 48(4), 801–816. Available from: <https://doi.org/10.1002/esp.5519>